Comparative Study of Gas Adsorption on Amorphous Ice: Thermodynamic and Spectroscopic Features of the Adlayer and the Surface

C. Manca,† C. Martin,‡ and P. Roubin*,‡

Department of Chemistry and Biochemistry, University of Bern, Freiestrasse 3, CH-3000 Bern 9, Switzerland, and Laboratoire Physique des Interactions Ioniques et Moléculaires UMR 6633, Université de Provence, Centre Saint Jérôme (service 242), F-13397 Marseille Cedex 20, France

Received: October 7, 2002; In Final Form: May 16, 2003

The features of adsorption on amorphous ice are compared for N_2, CO, Ar, Kr, CH_4, and CF_4, studied by both adsorption isotherm volumetry and infrared spectroscopy. The analysis of the two types of experimental results is consistent, allowing us to distinguish different behaviors according to the strength of the bonding with the ice surface sites. Adsorption energies and capacities have been estimated, and hydrogen bonding with surface dangling O−H has been evidenced for N_2 and CO. Infrared isotherms have been obtained for the three surface sites of ice and are compared with that of the adsorbate in the case of CH_4.

I. Introduction

Study of amorphous ice is relevant for the understanding of interstellar chemistry as it is the main part of the mantle covering grains in dusty clouds.[1] Numerous studies[2−6] have shown that amorphous ice has a large specific surface area and is then propitious to adsorption. Studies of adsorbate−ice interactions could be of great help for understanding reactivity and for deepening the knowledge of ice surface structure.

Infrared spectroscopy has been widely used to probe surface phenomena of amorphous ice,[7−14] and three types of surface molecules have been identified:[11,15,16] three-coordinated molecules having either a free OH group—called a dangling H site (dH)—or a free electronic pair on an oxygen atom—called a dangling O site (dO)—and four-coordinated molecules having a distorted H bond tetrahedron (s4). Their positions have been measured in the case of ice nanocrystals[17] respectively at 3692, 3560, and 3480 cm^{-1}. The first band is clearly observed out of the broad band at 3250 cm^{-1} (fwhm $\simeq$ 250 cm^{-1}) assigned to the OH stretching modes of bulk molecules, while the last two bands can be detected by performing difference spectra, using a probe molecule or annealing the sample to modify the spectral response of the corresponding surface sites.[18] In fact, some studies have compared the spectroscopic changes induced by different adsorbed molecules.[15,16,18−20] Conversely, very few studies have done a quantitative comparison of the adsorbed amounts, as is possible using adsorption isotherm volumetry.[4,21] Our experimental setup allows us to perform both types of measurements by simultaneously recording spectroscopic and volumetric data, and we have already shown the advantage in using the correlation between volumetric and infrared data by plotting *infrared isotherms*.[22] We are thus able to correlate the adsorbed amount and the vibrational modifications, to estimate adsorption energies and to determine the surface or nonsurface nature of infrared signals.

The purpose of this paper is to compare the adsorption of various gases on amorphous ice by infrared and volumetric comeasurements, to take advantage of each infrared isotherm that can be measured, and to analyze the origins of the different behaviors that we have observed. This paper is organized in three sections: experimental methods and models are detailed in section II, results obtained from volumetric and spectroscopic measurements as well as information deduced from their coupling are described in section III, and section IV is devoted to a general discussion.

II. Experimental Section

Volumetric isotherms and infrared measurements were simultaneously performed on a single sample inside a copper cell having two sapphire windows. The experimental setup is described in more detail in a previous work.[23] The temperatures indicated in this paper were determined by measuring the saturation pressure p^0 of the gas and using Clapeyron's law. Infrared spectra were collected using a Nicolet 7199 FTIR spectrometer. The resolution was 1 cm^{-1}, and 200 scans were collected per spectra.

Icy samples were prepared as follows: a gas mixture of H_2O/Ar (1:30) was promptly sprayed (rate of water molecules about 0.01 mol·h^{-1}) in the cell maintained at 40 K under a vacuum better than 10^{-4} Pa. At this temperature, both water and argon are trapped. The sample was then pumped and slowly annealed (0.2 K·min^{-1}) for about 5 h to 90 K, so that Ar could desorb and amorphous ice could be formed. Then, the sample (2−3 mg) was cooled to the temperature chosen for the isotherm; in these conditions, our samples are expected to be amorphous. It is well-known that ice structure strongly depends on its preparation conditions, and we therefore checked the amorphous nature of the sample by comparing the infrared spectrum at 90 K to those already published which were obtained in other conditions. As expected for amorphous ice, we measured large specific surface areas (more than 100 m^2·g^{-1}),[22] and N_2 isotherms performed at 56 K compare well with previous results.[3,4,24]

We performed point by point isotherms: for each step of the isotherm, we collected the value of the equilibrium pressure p to quantify the adsorbed amount and recorded an infrared spectrum to get the alterations in the signals of both ice and

* To whom correspondence should be addressed. E-mail: proubin@piima1.univ-mrs.fr.
† University of Bern.
‡ Université de Provence.

10.1021/jp022198a CCC: $25.00
Published on Web 08/06/2003

TABLE 1: Physical Properties and Experimental Conditions for the Different Adsorbates: Distance between Nearest Neighbors in the Condensed Phase, d_{nn}/nm, Temperature of the Critical Point, T_c/K, Saturation Pressure, p^0/Torr, Working Temperature, T/K, Ratio T/T_c, and Enthalpy of Condensation, $|\Delta_{cond}h|$/(kJ mol^{-1})

adsorbate	d_{nn}	T_c	p^0	T	T/T_c	$\lvert\Delta_{cond}h\rvert$
N_2	0.399	126.2	18.132	56.1	0.44	6.9
CO	0.399	132.9	7.534	57.0	0.43	8.3
Ar	0.376	150.9	5.330	59.8	0.40	7.9
Kr	0.401	209.4	2.056	77.8	0.37	11.0
CH_4	0.417	190.5	4.194	73.4	0.38	9.8
CF_4		227.7	2.205	94.5	0.41	13.6

adsorbate provided that the latter had an infrared-active mode. At the end of the experiment (i.e., when saturation pressure p^0 was reached), the adsorbate was desorbed. We checked that the ice surface had not been perturbed during adsorption by comparing the infrared spectra of bare ice before and after adsorption, and by performing an isotherm of CH_4, used here as a reference, before and after adsorption. The adsorbed amounts for the same equilibrium pressures were similar, showing that the ice surface had not been irreversibly altered during adsorption. When necessary, we compared results obtained with different ice samples by normalizing adsorbed amounts using those of reference CH_4 isotherms.

The probe molecules were nitrogen (Alpha Gaz, with a chemical purity of 99.9990%), carbon monoxide (Alpha Gaz, 99.997%), argon (Linde Gaz, 99.9996%), krypton (Linde Gaz, 99.990%), methane (Air Liquide, 99.95%), and tetrafluoromethane (Linde Gaz, 99.8%). These molecules provide good experimental conditions for 40 K < T < 100 K, the temperature range where amorphous ice remains stable.[25] They are nonchemically reactive and do not strongly perturb the ice surface: actually, only physisorption phenomena were observed, as is shown in the next part. In Table 1, we have reported their different sizes and electric properties: only CO has a dipole moment (0.121 D), and only CO and N_2 have a quadrupole moment (-9.47×10^{-40} and -4.65×10^{-40} C·m^2, respectively[26]).

At T < 15 K, gases such as N_2, CO, CH_4, and CF_4 form a separate solid film above the ice surface,[18] and we therefore checked that the chosen working temperatures allowed the gases to diffuse on the surface. They were also chosen to have analogous ratios T/T_c, T_c being the temperature of the critical point (Table 1), and we thus expected analogous thermodynamic conditions for all the adsorbates.

We used the Brunnauer, Emmet, and Teller (BET) model[27] to determine the monolayer capacity υ_m, BET constant C, and net heat of adsorption ΔQ, which represents the difference between the adsorption energy and the condensation energy. υ_m and C are two parameters which can be determined by plotting the linear transformed BET equation $p/[\upsilon^a(p - p^0)] = f(p/p^0)$, υ^a being the volume of adsorbed gas on the surface. ΔQ and the relative pressure at monolayer completion $(p/p^0)_m$ can be estimated using the following relations:

$$\Delta Q = RT \ln C \tag{1}$$

$$\left(\frac{p}{p^0}\right)_m = \frac{1}{C^{1/2} + 1} \tag{2}$$

C and $(p/p^0)_m$ give information on the strength of the interactions between the adsorbate and surface: the lower the $(p/p^0)_m$ value, the larger the C constant and the stronger the interactions. The calculated values of ΔQ are indicative only, but are useful to compare experiments performed at different temperatures.

According to results obtained on various materials,[28] the fit of the linear transformed BET equation is relevant only in a small range of relative pressure (0.05 < p/p^0 < 0.35 in the case of N_2), and BET values were calculated here taking great care of the pressure range used for the fit of data points for each adsorbate.

We also used the isosteric method to get the differential enthalpy of adsorption $\Delta_{ads}\dot{h}$: it consists of plotting a series of isotherms on the same ice sample at different temperatures. The equation relative to the gas−adsorbed phase equilibrium is analogous to that of Clausius−Clapeyron:

$$\Delta_{ads}\dot{h}_{(T,\upsilon a)} = R\left(\frac{\partial \ln p}{\partial (1/T)}\right)_{\upsilon a} \tag{3}$$

where R is the perfect gas constant, p the equilibrium pressure, and T is the working temperature. Assuming that $\Delta_{ads}\dot{h}$ is constant within the temperature range chosen (a few kelvin), ln p vs $1/T$ is linear and $\Delta_{ads}\dot{h}$ is the slope of the straight line. $|\Delta_{ads}\dot{h}| = q^{st}$ is the isosteric heat of adsorption, i.e., the heat produced by adsorption at the adsorbed amount υ^a. The value of ΔQ deduced from the BET method is an estimation of the mean value of $|\Delta_{ads}\dot{h}| - |\Delta_{cond}h|$ ($|\Delta_{cond}h|$ being the absolute value of the enthalpy of condensation) for the monolayer completion.

The correlation between the two techniques (adsorption isotherm volumetry and infrared spectroscopy) has been described elsewhere.[22] In short, it is performed by plotting the evolution in integrated absorbance of some selected bands versus the relative pressure and by normalizing them to make comparison with the evolution in adsorbed amount; we call the corresponding curves *infrared* and *volumetric* isotherms, respectively. Plotting the infrared isotherm may allow us to distinguish several components in the adsorbate signal:[23] a type I infrared isotherm means that the signal refers to monolayer molecules only, whereas a type II infrared isotherm means that the signal refers to both monolayer and multilayer molecules.

III. Results

A. Volumetric Isotherms. Figure 1a shows adsorption isotherms as functions of relative pressure for all the adsorbates. Except for CF_4, they are type II isotherms: the first part where υ^a rises and reaches a plateau corresponds to the monolayer completion; the second part, which is roughly linear, corresponds to the multilayer adsorption. In the third part when $p/p^0 \approx 1$, υ^a rises sharply, which corresponds to the formation of the condensed phase. In Figure 1b, the same isotherms are plotted on an extended scale to focus on the shape of their knee (i.e., the monolayer completion). The monolayer capacity υ_m and BET constant C deduced from the BET model are reported in Table 2. Considering the values of C, we can group the adsorbates into subclasses:

(1) adsorbates with large values of C (>200) and low values of $(p/p^0)_m$ (<0.1) (N_2 and CO); (2) adsorbates with low values of C (≤20) and large values of $(p/p^0)_m$ (>0.15) (Ar, Kr, CH_4); (3) adsorbates with no relevant value of C and $(p/p^0)_m$ (CF_4).

In the last case, the BET fit has revealed meaningless and nonconsistent values of υ_m have been obtained. As a matter of fact, the CF_4 isotherm does not present a knee at low values of relative pressure: this isotherm is type III and not type II, indicating nonattractive interaction with the surface and no wetting. The use of the BET model is therefore not appropriate, and the values obtained are not indicated in Table 2. It should

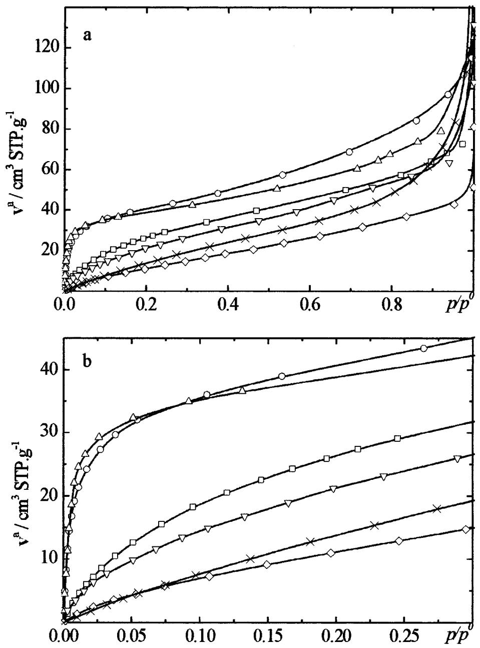

Figure 1. Volumetric isotherms on amorphous ice: (a) ○, N_2 (56 K); △, CO (57 K); ▽, Ar (60 K); ◇, Kr (78 K); □, CH_4 (73 K); ×, CF_4 (95 K); (b) same experimental points in the monolayer completion range (extended scale). Solid lines are guides for the eyes.

TABLE 2: BET Analysis of the Isotherms: Monolayer Capacity, v_m/(cm^3 STP g^{-1}), Reduced Monolayer Capacity, $\tilde{v}_m$, BET Constant, *C*, Relative Pressure at Monolayer Completion, $(p/p^0)_m$, and Net Heat of Adsorption, ΔQ/(kJ Mol^{-1})

adsorbate	v_m	$\tilde{v}_m$	C	$(p/p^0)_m$	ΔQ
N_2	33	1.33	218	0.06	2.5
CO	33	1.33	253	0.06	2.6
Ar	22	0.88	13	0.22	1.3
Kr	13	0.52	8	0.26	1.3
CH_4	25	1	20	0.18	1.8

be noted that this behavior is in agreement with the hydrophobic nature of CF_4.

For the other adsorbates, we have deduced the values of ΔQ from *C* using eq 1, with an accuracy of 0.2 kJ mol^{-1} (Table 2). These values are low, which confirms that the interactions between the adsorbates and ice surface are weak, and are in good agreement with previous results found with the same method for N_2,[2,29] Ar,[29] and CH_4[4] and with previous optical isotherm determinations for N_2,[18] CO,[13,18] and CH_4.[13]

We have recorded a series of five isotherms for at least one adsorbate of each subclass: N_2 (56−60 K), Ar (56−60 K), and CF_4 (95−99 K). Figure 2 shows the corresponding modifications in $|\Delta_{ads}\dot{h}| - |\Delta_{cond}h|$ as a function of v^a. The three curves are in agreement with what is expected, taking the type of the isotherms into account.[30] This plot allows us to compare the heat produced by adsorption with that produced by condensation, assuming that the variation of the entropic factor is negligible. In the case of CF_4, despite the large increase at low values of v^a, $|\Delta_{ads}\dot{h}| - |\Delta_{cond}h| < 0$, whatever the value of v^a, which means that adsorption is not energetically favored. On the contrary, in the case of N_2 and Ar, $|\Delta_{ads}\dot{h}| - |\Delta_{cond}h| > 0$, whatever the value of v^a. It is larger for N_2 than for Ar when $v^a \rightarrow 0$ (respectively at 3.2 and 0.5 kJ mol^{-1}), increases before the monolayer completion, reaching a maximum at 4.6 kJ mol^{-1} for N_2 and 1.9 kJ mol^{-1} for Ar, and then decreases to zero. These values are low, as those obtained by the BET method, and are in agreement with the expected weakness of interactions

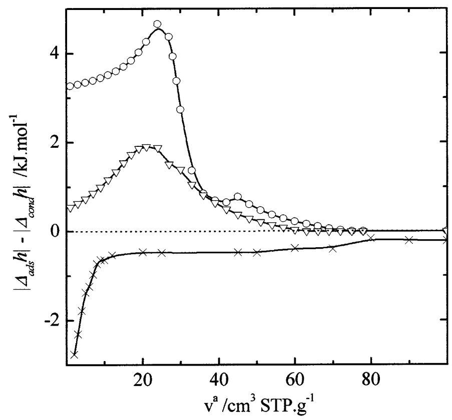

Figure 2. Differential enthalpy of adsorption minus condensation enthalpy, $|\Delta_{ads}\dot{h}| - |\Delta_{cond}h|$, vs adsorbed amount v^a: ○, N_2 (56−60 K); ▽, Ar (56−60 K); ×, CF_4 (95−99 K). Solid lines are guides for the eyes.

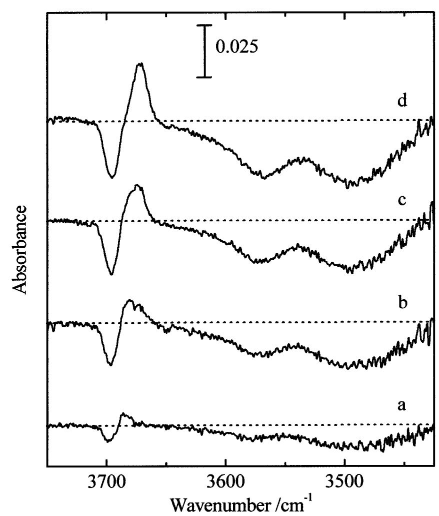

Figure 3. Infrared difference spectra of amorphous ice covered with CH_4 at 73 K for various surface coverages v^a/v_m: (a) 0.25, (b) 0.5, (c) 1, (d) 2 (the reference is bare ice at 73 K).

between the adsorbate and ice surface. The shape of the curves will be discussed in more detail in section IV.

In Table 2, we have also reported values of v_m and $\tilde{v}_m$, the latter being the ratio between the monolayer capacity measured for a gas and that measured for CH_4: $\tilde{v}_m$ depends on the adsorbate and ranges from 0.5 to 1.3, the largest capacity being found for CO and N_2. The values are in agreement with what Nair et al.[21] and Schmitt[29] have published in the case of Ar, N_2, and CO.

B. Infrared Spectra. During adsorption, changes are observed in the infrared spectrum of ice in the 3600−3450 cm^{-1} region. These changes cannot be directly detected and are revealed by subtracting the spectrum of bare ice before adsorption from the spectrum of ice covered with adsorbate. Negative (respectively positive) bands are associated with bands which decrease (respectively increase) during adsorption. Figure 3 shows these difference spectra for various surface coverages θ ($\theta = v^a/v_m$) of CH_4 at 73 K. Three bands decrease while only one band increases with surface coverage: the negative bands correspond to those previously mentioned in the Introduction and assigned to dH, dO, and s4 surface sites. The same behavior is observed for all the adsorbates as Figure 4 shows for monolayer completion. The band positions depend on the adsorbate and range from 3563 to 3576 cm^{-1} for dO and from 3488 to 3496 cm^{-1} for s4 (Table 3). An increasing dH band

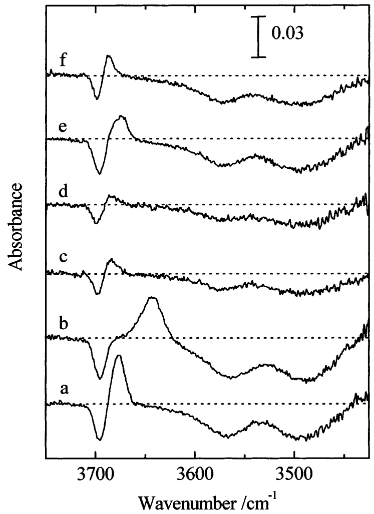

Figure 4. Infrared difference spectra of amorphous ice at monolayer completion (the reference is bare ice at the same temperature): (a) N_2 at 56 K, (b) CO at 57 K, (c) Ar at 60 K, (d) Kr at 78 K, (e) CH_4 at 73 K, (f) CF_4 at 95 K (spectra are raw data without normalization).

TABLE 3: Ice Surface Infrared Signals: Frequencies ν_{dH}/cm^{-1}, ν_{dO}/cm^{-1}, and ν_{s4}/cm^{-1}, Shift of the dH Band, $\Delta\nu_{dH}$/cm^{-1}, and Ratio of the Shifted dH Band Intensity vs That of the Original Free dH Band, A_{dH}/A_{dH0}

adsorbate	ν_{dO}	ν_{s4}	ν_{dH}	$\Delta\nu_{dH}$	A_{dH}/A_{dH0}
N_2	3567	3492	3674	−22	1.6
CO	3563	3488	3636	−60	2.1
Ar	3576	3493	3684	−12	1.0
Kr	3572	3495	3679	−17	0.9
CH_4	3571	3493	3672	−24	1.1
CF_4	3572	3496	3690	−6	0.9

corresponding to the decreasing dH band is clearly observed for all the adsorbates and is always red-shifted (from 6 to 60 cm^{-1}), whereas no positive signal is observed for dO and s4 signals. In fact, their width is larger than the expected shift of the signal due to adsorption; we thus assume that positive and negative components overlap in a large domain and no positive band is observed merely because their intensities are lower than those of initial dO and s4 bands.

We now focus on the positive dH signal: Figure 5 shows the free dH mode of bare ice and the shifted adsorption-induced modes for the different adsorbates at monolayer completion (it should be noted here that, as for Figure 4, these spectra are the raw data originating from various samples having various specific surface areas, and therefore, the relative intensities of the dH band cannot be compared directly in this figure). Each gas interacts with the dH groups, and this modifies the dH signal both in position and in intensity. The magnitude of the shift (Table 3) strongly depends on the adsorbate, the values being in agreement with those previously published.[8,18,19] The relative integrated intensities of the shifted dH mode (A_{dH}/A_{dH0}) are reported in Table 3. The largest ratios are measured for N_2 and CO (respectively 1.6 and 2.1), while they are roughly 1 for Ar, Kr, CH_4, and CF_4, a similar adsorbate enhancement of the infrared intensity already being observed for N_2 and CO.[18] Rozenberg et al.[20] have calculated the enthalpy of the hydrogen bond ΔH thanks to Iogansens's "rule of intensity",[31] using the difference of the integrated absorbance of a mode before (here A_{dH0}) and after (A_{dH}) the formation of the hydrogen bond:

$$\Delta H = -K({A_{dH}}^{1/2} - {A_{dH0}}^{1/2}), \qquad K > 0 \tag{4}$$

We are not able to reproduce such calculations since we cannot calculate the number of water molecules that we probe with the infrared beam and since we do not know exactly the infrared cross sections of the signals. Nevertheless, the ratio A_{dH}/A_{dH0} provides qualitative information: if $A_{dH}/A_{dH0} > 1$ (respectively $A_{dH}/A_{dH0} < 1$), $\Delta H < 0$ (respectively $\Delta H > 0$) and a hydrogen bond (respectively no hydrogen bond) is formed with dangling OH. We can therefore group the molecules into subclasses here: (1) molecules with $A_{dH}/A_{dH0} > 1$ (N_2 and CO); (2) molecules with $A_{dH}/A_{dH0} \simeq 1$ or < 1 (Ar, Kr, CH_4, and CF_4).

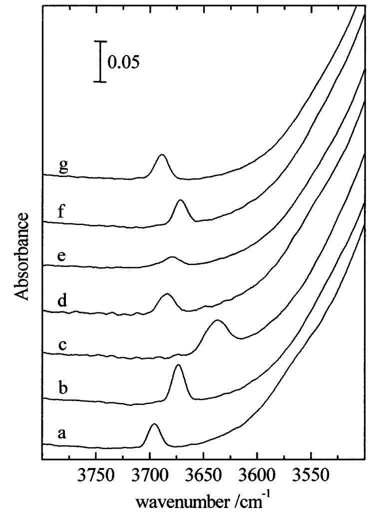

Figure 5. Infrared spectrum in the ν_{dH} region of bare ice (a) and those of ice covered with an adsorbate at monolayer completion: (b) N_2 at 56 K, (c) CO at 57 K, (d) Ar at 60 K, (e) Kr at 78 K, (f) CH_4 at 73 K, (g) CF_4 at 95 K (spectra are raw data without normalization).

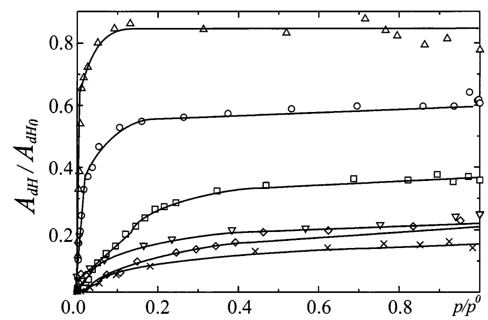

Figure 6. Infrared isotherms of the shifted ν_{dH} band of ice: ○, N_2 (56 K); △, CO (57 K); ▽, Ar (60 K); ◇, Kr (78 K); □, CH_4 (73 K); ×, CF_4 (95 K). Solid lines are guides for the eyes.

C. Correlation between the Two Techniques. Figure 6 shows the infrared isotherms deduced from the shifted dH mode evolution for each adsorbate. They are all type I isotherms: absorbance rises at low values of p/p^0 and then reaches a horizontal plateau; this confirms the pure surface origin of the dH band. It should be noted that the shape of the knee of these type I isotherms depends on the adsorbate in the same manner as that of the type II volumetric isotherms shown in Figure 1.

Infrared isotherms can also be plotted using the integrated absorbance of the two other surface-localized modes, dO and s4. Figure 7 shows the whole isotherms that we can plot for CH_4, volumetric and infrared, three from ice (dH, dO, and s4) and one from CH_4 (the stretching mode ν_3), the infrared isotherms being scaled to compare them to the volumetric isotherm. The most striking feature is that the methane isotherm is type II as is the volumetric isotherm whereas the ice isotherms are type I. This reveals that the ν_3 signal contains both surface and multilayer contributions that cannot be distinguished.[22] A similar study has been detailed in the case of CO[23] where two stretching bands are observed and the plots of infrared isotherms

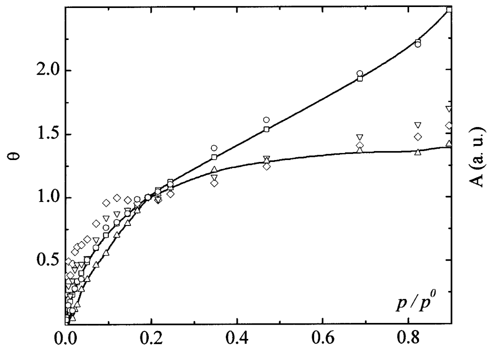

Figure 7. Volumetric isotherm (surface coverage $\theta = v^a/v_m$) and infrared isotherms (normalized integrated absorbance A) in the case of CH_4 adsorbed on amorphous ice: □, volumetric; ○, CH stretching mode of CH_4 and surface-localized modes of ice; △, dH; ▽, dO; ◇, s4. Solid lines are guides for the eyes.

have allowed us to distinguish a pure surface CO signal from a mixed surface multilayer CO signal. It should be noted that the differences observed in the shape of the knee of the various isotherms plotted in Figure 7 are within the accuracy of the integrated absorbance measurements, which is due to the width and the overlap of the bands, especially in the case of dO and s4. The shapes of the first part of all the isotherms are roughly similar, and this is observed in the same manner for all the other gases, indicating that the adsorption energies are roughly similar for the three surface sites. Adsorption energies have been calculated for the three sites in the case of CO[23] respectively at 11.4, 10.6, and 9.6 kJ mol^{-1} for dH, dO, and s4.

IV. Discussion

The measured values of adsorption energies deduced from BET modeling as well as from the difference $|\Delta_{ads}\dot{h}| - |\Delta_{cond}h|$ are weak (less than 3 kJ mol^{-1}), and this proves that only weak interactions are involved in these adsorption phenomena. These values are nevertheless clearly larger for N_2 and CO than for the other adsorbates, and we will discuss here the various contributions evidenced by our experiments to explain their specific behavior. Thermodynamic results (section III, part A) as well as spectroscopic results (section III, part B) have evidenced three subclasses of adsorbates, grouping first N_2 and CO, second Ar, Kr, and CH_4, and finally CF_4. N_2 and CO have the largest values of the BET constant C (i.e., of ΔQ), the largest values of the adsorbed amount v_m (Table 2), and the strongest bonding with dH sites via the formation of a hydrogen bond: all these results are consistent with the existence of specific interactions leading to a higher affinity with ice. Hydrogen bonding between ice and adsorbate should contribute to the high value of the adsorption energy, but there is probably another contribution, N_2 and CO also being the lone molecules having a quadrupole moment. In a previous work,[23] periodic DFT calculations have modeled CO adsorption on ice and L-type CO:CO structures have been proved to match the ice surface, leading to stabilizing lateral CO−CO interactions. The same type of phenomenon is expected for N_2, and quadrupole−quadrupole interaction thus probably contributes to the adsorption energy measured in the case of N_2 and CO.

In addition, these nonspherical molecules may interact perpendicularly at the surface, especially with free hydroxyl groups,[32,33] their cross-sectional area getting smaller. In the case of N_2, it has been shown that the cross-sectional area can decrease from 0.162 to 0.112 nm^2 at 77 K.[28] In fact, this has been confirmed by our calculations in the case of CO,[23] half of the adsorbed molecules being roughly perpendicular to the surface, and this explains the large monolayer capacity measured for these two gases.

Concerning spherical adsorbates (Ar, Kr, and CH_4), the values of $\tilde{v}_m$ (Table 2) are not correlated to distances between nearest neighbors in the solid phase, d_{nn} (Table 1): for example, the Ar adsorption capacity is lower than that of CH_4 although d_{nn} is lower. The three molecules have similar sizes and similar values of T/T_c and are expected to have similar mobilities and to explore the same volume of the sample: the difference in the adsorbed amount therefore shows a difference in the monolayer coverage, the density of the adlayer also being different from that of the condensed phase. This proves that, despite the weakness of the interactions between the adsorbate and ice, the ice surface constrains a specific adlayer structure.

The adsorption energy has been correlated here to the enhancement of the dangling OH mode intensity, but it should be noted that, conversely, it cannot be correlated to its frequency shift. The adsorption of CO leads to the largest shift (60 cm^{-1}) as well as the largest value of ΔQ, but the adsorption of N_2, which behaves as CO, leads to a shift that compares to those of Kr or CH_4 (roughly 20 cm^{-1}), which are low interacting molecules (see Tables 2 and 3). Periodic Hartree−Fock calculations have been developed and have shown[34] that the frequency shift of the dangling OH bond is due to a vibrational Stark effect and thus has its origin in the modification induced by adsorption of the electric properties at the surface. This emphasizes the role of the electric field at the ice surface, which is high, being of the same order of magnitude ($\sim 10^9$ V·m^{-1}) as for ionic surfaces such as those of MgO and zeolites. This also points out that merely correlating the shift of an infrared mode and the strength of an interaction may be wrong, even in the case of an uncoupled stretching.

The different behaviors of the adsorbates are also clearly evidenced by the plot of $|\Delta_{ads}\dot{h}| - |\Delta_{cond}h|$ as a function of the surface coverage (section III, part A, and Figure 2). Positive values prove that N_2 and Ar wet the surface, whereas negative values prove that CF_4 does not wet the surface. In this last case, the layer growth is probably achieved by three-dimensional clustering on the surface, in agreement with the calculations performed by Devlin et al.:[18] a top view of the cluster of water molecules clearly shows that CF_4 does not cover the dH groups, as expected taking the hydrophobic nature of CF_4 into account. We have checked clustering by obtaining infrared spectra of CF_4 isolated in an argon matrix for different concentrations and by comparing them to that of CF_4 adsorbed on ice and to that of solid CF_4 (Figure 8). The signal of adsorbed CF_4 is taken here at monolayer completion, its shape remaining identical for all the stages of adsorption. The modification of the signal of CF_4 isolated in argon from 1:1000 to 1:10 is consistent with the formation of clusters with increasing the concentration: a broad band centered at 2155 cm^{-1} appears for c = 1:20 and shifts toward lower frequency, getting close to that of solid CF_4 at higher concentration. It is therefore obvious that the signal of adsorbed CF_4 is close to that of CF_4 clusters.

For N_2 and Ar, $|\Delta_{ads}\dot{h}| - |\Delta_{cond}h|$ increases at the beginning of adsorption, giving evidence for lateral stabilizing interactions, and reaches a maximum for coverage close to that of the full monolayer. The value for $v^a = 0$ is much larger for N_2 (3.2 kJ mol^{-1}) than for Ar (0.5 kJ mol^{-1}), whereas the magnitude of the increase is the same (1.4 kJ mol^{-1}) for the molecules. These values can be compared to energy values related to dimers or complexes: at the beginning of adsorption, the molecule is isolated on the surface and the interaction may be compared to that of the 1:1 complex with H_2O, whereas for coverage higher

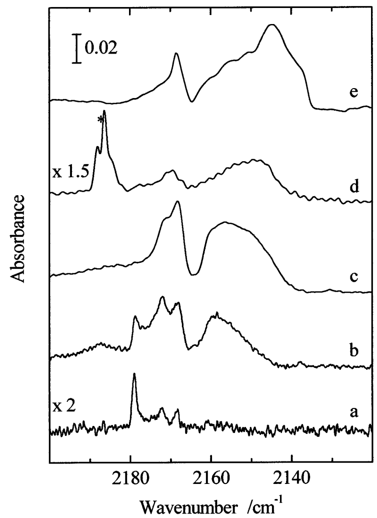

Figure 8. Infrared spectra of CF_4 ($\nu_1 + \nu_3$): (a) isolated in argon, $T = 20$ K, $c = 1{:}1000$, (b) isolated in argon, $T = 20$ K, $c = 1{:}20$, (c) isolated in argon, $T = 20$ K, $c = 1{:}10$, (d) adsorbed on ice, $T = 95$ K (the asterisk indicates the gas phase), (e) solid, $T = 60$ K.

but less than the full monolayer, lateral molecule−molecule interaction occurs which may be compared to that of the dimer. As a matter of fact, for a 1:1 complex, N_2 interacts more strongly with H_2O than Ar (its energy is calculated with the same method[35] at 440 and 132 cm^{-1}, respectively), and conversely, the Ar dimer[36] and the N_2 dimer[37] have similar energies (~100 cm^{-1}). It should be noted that Franken et al.[37] have also calculated the energy of the N_2:H_2O complex, at 383 cm^{-1}, which is in agreement that of ref 35. These authors have also determined another stable complex, only 37 cm^{-1} less stable, forming a conventional hydrogen bond, where one O−H bond is directed toward the end of the nitrogen molecule, this structure having been observed experimentally.[38] This is consistent with the evidence for hydrogen bonding found in our results.

V. Conclusion

We have compared the adsorption of several gases (N_2, CO, Ar, Kr, CH_4, and CF_4) on amorphous ice using both adsorption isotherm volumetry and infrared spectroscopy. These gases weakly interact with ice, and only physisorption phenomena are observed: we have actually measured an interaction energy of less than 3 kJ mol^{-1}. Both methods have allowed us to distinguish three classes of molecules: N_2 and CO, which interact with dangling OH via a hydrogen bond, Ar, Kr, and CH_4, for which interactions with ice are weak but attractive and which form a monolayer, and finally CF_4, which does not wet the surface, growing by forming three-dimensional clusters. We have evidenced the existence of stabilizing lateral interactions during the formation of the monolayer of the same order of magnitude for all the gases. On the other hand, for molecule having a quadrupole moment, the large capacity of the monolayer has been interpreted as due to the good matching between the ice surface and the adlayer, allowing the formation of L-type configurations for the adsorbed molecules. Spectroscopic and volumetric measurements have revealed a good consistency, especially in showing that the strength of the interaction between ice and adsorbate should be related to the magnitude of the infrared intensity of the dangling OH mode rather than to its frequency shift.

References and Notes

(1) Schmitt, B. Molecules and grains in space, 50th international meeting of physical chemistry, Mt. Saint-Odile, France, September 1993.
(2) Ghormley, J. A. *J. Chem. Phys.* **1967**, *46*, 1321.
(3) Mayer, E.; Pletzer, R. *Nature* **1986**, *319*, 298.
(4) Schmitt, B.; Ocampo, J.; Klinger, J. *J. Phys.* **1987**, *48*, C1.
(5) Pletzer, R.; Mayer, E. *J. Chem. Phys.* **1989**, *90*, 5207.
(6) Stevenson, K. P.; Kimmel, G. A.; Dohnalek, Z.; Smith, R. S.; Kay, B. D. *Science* **1999**, *283*, 1505.
(7) Rowland, B.; Fisher, M.; Devlin, J. P. *J. Chem. Phys.* **1991**, *94*, 812.
(8) Buch, V.; Devlin, J. P. *J. Chem. Phys.* **1991**, *94*, 4091.
(9) Rowland, B.; Fisher, M.; Devlin, J. P. *J. Chem. Phys.* **1991**, *95*, 1378.
(10) Devlin, J. P. *J. Phys. Chem.* **1992**, *96*, 6185.
(11) Devlin, J. P. *Physics and Chemistry of Ice*; Maeno, N., Hondoh, T., Eds.; Hokkaido University Press: Sapporo, 1992; p 183.
(12) Schaff, J. E.; Roberts, J. T. *J. Phys. Chem.* **1994**, *98*, 6900.
(13) Allouche, A.; Verlaque, P.; Pourcin, J. *J. Phys. Chem. B* **1998**, *102*, 89.
(14) Borget, F.; Chiavassa, T.; Allouche, A.; Aycard, J. *J. Phys. Chem. B* **2001**, *105*, 449.
(15) Delzeit, L.; Devlin, M. S.; Rowland, B.; Devlin, J. P.; Buch, V. *J. Phys. Chem.* **1996**, *100*, 10076.
(16) Devlin, J. P.; Buch, V. *J. Phys. Chem. B* **1997**, *101*, 6095.
(17) Rowland, B.; Kadagathur, N. S.; Devlin, J. P.; Feldman, T.; Wojcik, M. J. *J. Chem. Phys.* **1995**, *102*, 8328.
(18) Devlin, J. P.; Buch, V. *J. Phys. Chem.* **1995**, *99*, 16534.
(19) Sadlej, J.; Rowland, B.; Devlin, J. P.; Buch, V. *J. Chem. Phys.* **1995**, *102*, 4804.
(20) Rozenberg, M.; Loewenschuss, A.; Marcus, Y. *Langmuir* **1999**, *15*, 5454.
(21) Nair, N.; Adamson, A. *J. Phys. Chem.* **1970**, *74*, 2229.
(22) Manca, C.; Roubin, P.; Martin, C. *Chem. Phys. Lett.* **2000**, *330*, 21.
(23) Manca, C.; Martin, C.; Allouche, A.; Roubin, P. *J. Phys. Chem. B* **2001**, *105*, 12861.
(24) Ghormley, J. A. *J. Chem. Phys.* **1968**, *48*, 503.
(25) Manca, C.; Martin, C.; Roubin, P. *Chem. Phys. Lett.*, in press.
(26) Graham, C.; Imrie, D. A.; Raab, R. E. *Mol. Phys.* **1998**, *93*, 49.
(27) Brunauer, S.; Emmet, P.; Teller, E. *J. Am. Chem. Soc.* **1938**, *60*, 309.
(28) Rouquerol, F.; Rouquerol, J.; Sing, K. *Adsorption by powders & porous solids*; Academic Press: London, 1999.
(29) Schmitt, B. Ph.D. Thesis, Université scientifique technologique et médicale, 1986.
(30) Sing, K. S. W.; Ramakrishna, V. R. *Colloques internationaux du CNRS, n°201-Thermochimie*, éditions du CNRS, Paris, 1972.
(31) Iogansen, A. V. *Spectrochim. Acta* **1999**, *A55*, 1585.
(32) Rouquerol, J.; Rouquerol, F.; Pérès, C.; Grillet, Y.; Boudellal, M.; Imelik, B. *Characterization of porous solids*; London Society of Chemical Industry: London, 1979.
(33) Rouquerol, J.; Grillet, Y.; Torralvo, M. J. *Fundamental of adsorption*; Engineering Foundation: New York, 1984.
(34) Manca, C.; Allouche, A. *J. Chem. Phys.* **2001**, *114*, 4226.
(35) Visagin, A. A. *J. Quant. Spectrosc. Radiat.* **2000**, *64*, 25.
(36) Zhang, Y. Z.; Pei, W.; Yang, W. *J. Chem. Phys.* **1997**, *107*, 7921.
(37) Franken, K. A.; Dykstra, C. E. *J. Phys. Chem.* **1993**, *97*, 11408.
(38) Leung, H. O.; Marshall, M. D.; Suenram, R. D.; Lovas, F. J. *J. Chem. Phys.* **1989**, *90*, 700.